Self-Assembled Topological Insulator: Bi_2Se_3 Membrane as a Passive Q-Switcher in an Erbium-Doped Fiber Laser

Yu Chen, Chujun Zhao, Huihui Huang, Shuqing Chen, Pinghua Tang, Zhiteng Wang, Shunbin Lu, Han Zhang, Shuangchun Wen, and Dingyuan Tang

***Abstract*—We demonstrate a new type of optical saturable absorber based on the self-assembled topological insulator Bi_2Se_3 membrane fabricated by the drop-cast/evaporation approach. The strong viscosity of Bi_2Se_3 allows its attachment onto the optical fiber end-facet for practical optoelectronic applications. The balanced twin-detector technique was used to characterize the saturable absorption parameters of the device, which has a saturating intensity of 101.8 MW/cm^2 and a modulation depth of 41.2% at the telecommunication band. By deploying this device into a fiber laser cavity, we had achieved stable Q-switched pulses with a repetition rate of 8 kHz and pulse duration of 14 μs. Through fine tuning the laser pump strength and/or cavity birefringence, we could widely change the Q-switched pulse repetition rate from 4.508 kHz to 12.88 kHz, pulse duration from 13.4 μs to 36 μs, and lasing wavelength from 1545.0 nm to 1565.1 nm. A dual-wavelength passive Q-switching operation was also obtained by enhancing the intra-cavity birefringence. Our results show the effectiveness of developing Bi_2Se_3 optical saturable absorber device by the drop-cast/evaporation method and applications for pulsed laser operation.**

***Index Terms*—Dual-wavelength laser, fiber laser, Q-switching, topological insulator.**

I. Introduction

TOPOLOGICAL INSULATOR (TI), a quantum phase of matter featured by a metallic surface state wherein a single Dirac cone arises from the symmetry breaking and a narrow-band-gap insulating bulky state, is expected to show unique photonics properties owing to its broadband spectral response ranging from terahertz to infrared as a result of the intrinsic gapless surface band, in analogy to graphene [1] and strong spin-orbital coupling effect that may lead to novel opto-spintronic devices [2]. Bi_2Se_3, Bi_2Te_3 and Sb_2Te_3 are typical examples of three dimensional topological insulators even under ambient condition. Despite that their electromagnetic properties had been extensively investigated [3]–[7], their equally interesting optical properties were under very limited studies. In the meanwhile, they possess different physical and chemical properties, such as band gap, band structure, Fermi energy level and carrier density [8]–[10], leading to new insights on photonics, which deserves further exploration by the optics community.

Passively Q-switched fiber lasers had attracted much attention because of their potentials as compact, simple, flexible, stable sources in medicine, laser processing, telecommunications, and remote sensing. They had been investigated intensively using different kinds of saturable absorbers (SAs), such as Sm-doped fiber [11], Er ions themselves [12], metal-doped crystals [13], [14], semi- conductor quantum well structures [15], and carbon nanotube [16]. However, due to some intrinsic drawbacks of those SAs, such as free space alignments, complex fabrication process required, limited operation bandwidth, their applications are limited. Recently, graphene, a single two-dimensional atomic layer Dirac materials of carbon atom arranged in a hexagonal lattice as the next-generation passive Q-switcher emerges, with the advantage of ultrafast recovery time and broadband saturable absorption [17]–[22]. The advancement in graphene SA renders us to raise a fundamental but interesting question, whether other type of Dirac material topological insulator could also exhibit saturable absorption?

Quite recently, based on the open and close aperture z-scan measurement at 800 nm under femtosecond laser illumination, we could unambiguously identify the real and imaginary part of the third-order nonlinear optical property of topological insulator: Bi_2Se_3, having large nonlinear refractive index and saturable absorption, respectively [23]. The experimental results demonstrated that Bi_2Se_3 could be a promising nonlinear optical material with applications ranging from the ultra-fast laser photonics (as a saturable absorber (SA) device for example) to the nonlinear Kerr photonics (as a thin film Kerr medium for optical switching, signal processing *etc*.). The ability of TI-based SA devices for ultra-fast pulse lasers was demonstrated in [24]–[26], in which a TI on a quartz substrate was employed as a SA device. To overcome the drawbacks owing to the quartz substrate, such as insertion loss and random reflection, in this work, a TI-based SA sandwiched by optical fiber pigtails was further fabricated through first drop-casting

Manuscript received May 02, 2013; revised June 23, 2013 and July 11, 2013; accepted July 13, 2013. Date of publication July 16, 2013; date of current version August 05, 2013. This work is supported in part by the National 973 Program of China (Grant No. 2012CB315701), in part by the National Natural Science Foundation of China (Grant Nos. 61025024 and 61222505), in part by the Program for New Century Excellent Talents in University of China (Grant No. NCET 11-0135), and in part by Hunan Provincial Natural Science Foundation of China (Grant No. 12JJ7005).

Y. Chen, C. Zhao, H. Huang, S. Chen, P. Tang, Z. Wang, S. Lu, H. Zhang, and S. Wen are with Key Laboratory for Micro-/Nano- Optoelectronic Devices of Ministry of Education, College of Physics and Microelectronic Science, Hunan University, Changsha 410082, China (e-mail: hanzhang@hnu.edu.cn).

D. Tang is with School of Physics and Electronic Engineering, Jiangsu Normal University, Xuzhou 221116, China (e-mail: tangdingyuan@jsnu.edu.cn).

Color versions of one or more of the figures in this paper are available online at http://ieeexplore.ieee.org.

Digital Object Identifier 10.1109/JLT.2013.2273493

and then evaporation approach. We characterized its nonlinear optical response by the balanced twin-detector technique and identified that its saturating intensity is about 101.8 MW/cm^2 and modulation depth is about 41.2%. By taking advantage of this saturable absorption property, we have achieved either single wavelength or dual-wavelength Q-switched operation from an erbium-doped fiber laser.

II. Result and Discussion

A. Topological Insulator Q-Switcher

1) Material Preparation: Two representative approaches, top-down exfoliation from bulk materials and bottom-up synthesis from chemical molecular groups, are generally used for the fabrication of nano-material based optoelectronic devices [29]. Herein, we used the bottom-up method: the Bi_2Se_3 nano-platelets (NPs) synthesized via a polyol method [27]. The as-prepared Bi_2Se_3 nano-sheets were dispersed in isopropyl alcohol and ultrasonicated for 6 hours. The Bi_2Se_3 dispersion solution in isopropyl alcohol was then dropped cast directly onto the fiber end-facet, while the fiber is inserted in a standard FC/PC fiber connector. After drying at 80°C for over two hours, the Bi_2Se_3 molecules could be self-assembled onto the fiber end-facet thanks to the strong viscosity of Bi_2Se_3. By connecting this Bi_2Se_3-on-fiber component with another clean and dry FC/PC fiber connector, the TI-based-SA device was thereby constructed for fiber laser application.

2) Characteristics of the Bi_2Se_3 Sample: As can be seen in Fig. 1(a), part of the fiber end-facet (including the outer cladding with a diameter of $\sim$125 μm and inner core with a diameter of $\sim$9 μm), especially the fiber core area is fully covered by the TI sample. The TEM image of the as-prepared Bi_2Se_3 is shown in Fig. 1(b), distinct layered constructions of the Bi_2Se_3 could be seen from the image. The layered Bi_2Se_3 implies the high surface to volume ratio which highlights the effects of the surface states in the 3D TI materials that are directly related to their topological properties. Fig. 1(c) compares the Raman spectrum of the layered and bulk Bi_2Se_3 in the range of 50–200 cm^{-1}using the 488 nm excitation line at room temperature by a Horiba-Jobin-Yvon Lab Raman HR confocal microscope. Three typical Raman peaks of Bi_2Se_3 centered at $\sim$70 cm^{-1}, $\sim$130 cm^{-1} and $\sim$173 cm^{-1}, were found in both of the spectra, which are correlated with the out-plane vibrational modA_{1g}^1, in-plane vibrational mode E_g^2 and the out-plane vibrational modeA_{1g}^2 of Se-Bi-Se-Bi-Se lattice vibration, respectively [28]. The intensity of theA_{1g}^1 in the layered Bi_2Se_3 spectrum is relatively stronger than that in the bulky Bi_2Se_3 spectrum. Furthermore, the line widths of the Raman peaks in the layered Bi_2Se_3 spectrum are a little bit broader than that in the bulk Bi_2Se_3 spectrum, which also confirms its layered structures [27]. It is worth noting that the E_g^1mode of Bi_2Se_3 remained unrevealed in this work due to the limitation of the spectrometer. The nearly flat linear absorption in the near-infrared wavelength band in Fig. 1(d) clearly shows that the Bi_2Se_3 sample has a broadband optical response at the telecommunication band. The insert left shows Bi_2Se_3 dispersion solution in isopropyl alcohol after ultra-sonication and right shows that Bi_2Se_3 occupies almost the entire fiber end-facet. Noting that the TI: Bi_2Se_3 on the fiber facet was not very uniform, the sample would cause the beam quality degradation of single mode fiber (SMF). The measured output beam profile for the fiber without (a) or with (b) TI using a high resolution Charge-coupled Device (CCD) is shown in Fig. 2. As it can be seen, the beam quality was not under serious degradation, which may decrease the coupling efficiency into another SMF. We had measured the total insertion loss of the TI saturable absorber device, which is about 3.1 dB.

In order to characterize the nonlinear optical response of the as-fabricated saturable absorber device, we performed the balanced twin-detector measurement at telecommunication wavelength, using the experimental setup shown in Fig. 3(a). A stable pulse train was emitted from a home-made passively mode-locked laser source (repetition rate: 1.754 MHz, central wavelength: 1568.5 nm and 3 dB bandwidth: 2.16 nm, pulse width: 1.97 ps, maximum power before the sample: 3.82 mW, correspondingly, maximum incident intensity: 1.738 GW/cm^2). We could control the input power by adjusting the tunable attenuator connected to the source directly. After passing through a 3-dB coupler, the output light was equally separated into two laser beams with almost identical strength. We let one laser beam pass through the sample, which was then measured by the photodiode detector A, while the other laser beam as a reference beam was directly measured by another photodiode detector B. These two detectors were connected with a dual-channel power meter (Newport 2936-C), which synchronously measured the input and output pulse intensity and hence effectively reduced the detection errors. Through continuously adjusting the incident power, a series of the output powers versus the input powers for the sample was detected by the dual-channel power meter, and consequently the optical transmittance under different input power was recorded.

Fig. 3(b) shows the nonlinear transmission curve. The curve was fitted with the following equation:

$$T(I) = 1 - \Delta T * \exp(-I/I_{\rm sat}) - T_{\rm ns}$$

where $T(I)$ is the transmission, ΔT is the modulation depth, I is the input intensity, $I_{\rm sat}$ is the saturating power density, and $T_{\rm ns}$ is the non-saturable absorbance. Upon fitting the measured experimental data by the above equation, we can infer that the saturating intensity is about 101.8 MW/cm^2 and the modulation depth is about 41.2%.

To further verify whether the measured saturable absorption is intrinsically caused by Bi_2Se_3 itself, we conducted three comparative experiments. (1) Continuously increasing (case 1 and case 3) (resp. decreasing (case 2 and case 4)) the input power from low (resp. high) to high (resp. low) power at different time, both nonlinear transmittance curves are satisfactorily overlapped within the detection limit, as shown in Fig. 3(c) and (d). (2) Comparing the nonlinear transmittance curves under different time before (Fig. 3(b), (c)) and after (Fig. 3(d)) the TI-SA was inserted into the laser cavity as Q-switcher, the inferred nonlinear absorption parameters (saturating intensity and modulation depth) are kept almost constant, as illustrated in Fig. 3(b), (c), (d) and Table I. (3) Replacing the fiber pigtailed Bi_2Se_3 with a fresh and un-used fiber pigtail,

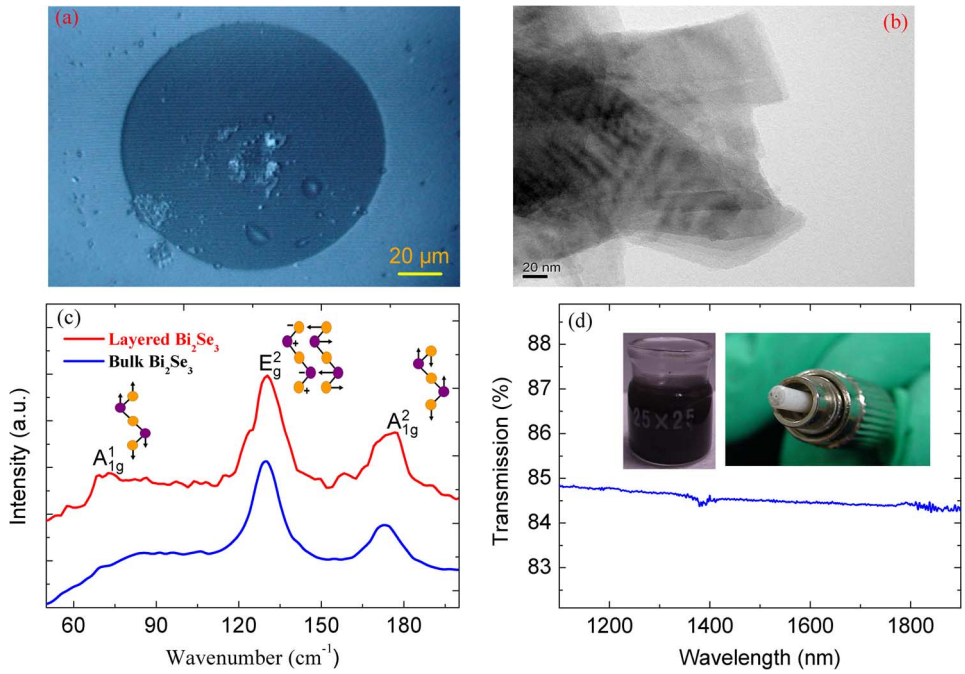

Fig. 1. (a) Optical image of the fiber end-facet (diameter 125 μm) covered with Bi_2Se_3. (b) TEM image of the layered Bi_2Se_3. (c) Raman spectra of the layered Bi_2Se_3 and bulky Bi_2Se_3. (d) The near infrared linear absorption spectra of Bi_2Se_3. Insert: Bi_2Se_3 dispersion solution in isopropyl alcohol after ultra-sonication (left) and photograph of a fiber pigtail coated with Bi_2Se_3 on the fiber end-facet (right).

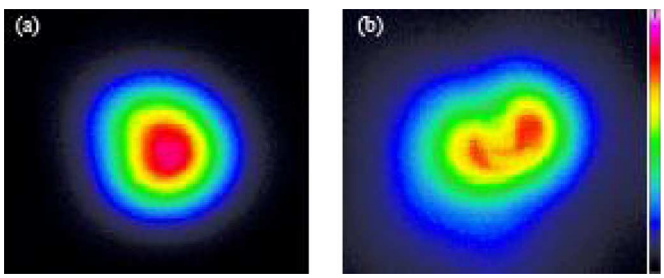

Fig. 2. The measured beam profile for the fiber (a) without TI and (b) with TI sample.

we could only observe a flat curve as shown in the insert of Fig. 3(b). Noting that these nonlinear transmittance curves were measured before and after the TI-SA was inserted into cavity as Q-switcher, we can know that the Bi_2Se_3 layers have not been damaged after they were connected with another FC/PC fiber connector. Based on these experiments, we are able to conclude that the measured saturable absorption characteristics are indeed contributed by Bi_2Se_3 other than some artifices, such as measurement errors, optical damage effect from Bi_2Se_3.

Through the designed comparative experiments above, we could also roughly estimate the laser intensity that this device could endure. We increased the input power to the maximum, and then measured the data with decreasing input power. It was found that even at the maximum input power of 3.82 mW, which corresponds to an input intensity of 1.738 GW/cm^2, the nonlinear transmittance curves before and after the maximum input laser illumination did not show obvious difference. And more importantly, through comparing the optical transmittance loss under different conditions, we found that it was almost kept constant. These experimental results show that the Bi_2Se_3 device could withstand an optical intensity larger than 1.738 GW/cm^2 without optical damage, indicating that it is suitable for high power laser applications. However, to preciously characterize the laser damage threshold of Bi_2Se_3, one needs to employ the single-shot damage threshold measurement technique that was previously used to study the chemical vapor deposition graphene [30].

B. Q-Switched Fiber Laser

The experimental setup is sketched in Fig. 4. The total cavity length is about 34.7 m, which consists of a piece of 1 m highly-doped erbium-doped fiber (EDF, LIEKKI Er80-8/125) with group velocity dispersion (GVD) of -20 ps^2/km, a total length of 25 m single mode fiber (SMF) with GVD of -23 ps^2/km and several pieces of passive fibers for connecting the components. The laser is pumped by a laser diode source of wavelength 975 nm, a 980/1550 wavelength-division multiplexer (WDM) is used to couple the pump light into the cavity and a 10% fiber coupler is employed for the output of the signal. A polarization-independent isolator (PI-ISO) is used to force the unidirectional operation of the ring cavity, and a polarization controller (PC) is used to fine adjust the cavity birefringence. An optical spectrum analyzer (Ando AQ-6317B) with spectral resolution of 0.015 nm and a 500 MHz oscilloscope (Tektronix TDS3054B) combined with a 5 GHz photo-detector (Thorlabs SIR5) are employed to simultaneously monitor the laser spectra and output pulses.

Firstly, we tested the operation characteristic of the fiber laser without incorporating the TI-SA. Only the continuous-wave (CW) emission was obtained even when the pump strength and cavity polarization were tuned in a wide range. This experiment excluded the possibility of self-Q-switching of the laser. Later,

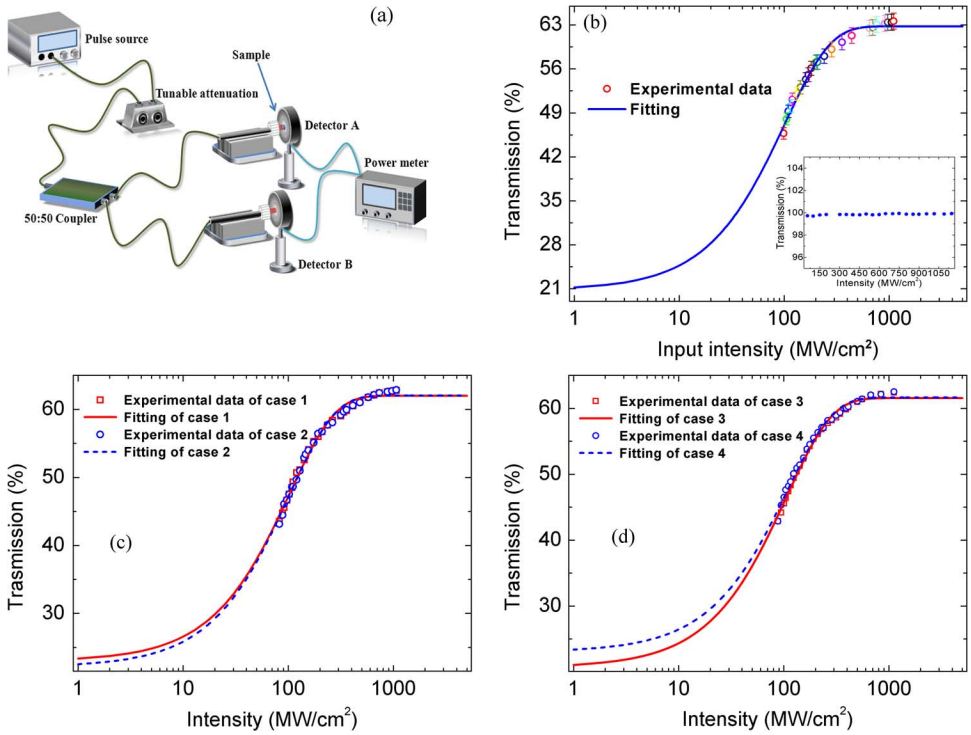

Fig. 3. (a) Experimental setup of the balanced twin-detector measurement technique. (b) The measured saturable absorption data and its corresponding fitting curve. Insert: the optical transmittance under different input powers but the fiber pigtailed Bi_2Se_3 is replaced with a fresh and un-used fiber pigtail. (c) The saturable absorption data measured by continuously increasing (case 1) and decreasing (case 2) the input power at different time A. (d) The saturable absorption data measured by continuously increasing (case 3) and decreasing (case 4) the input power at different time B.

TABLE I
THE INFERRED NONLINEAR ABSORPTION PARAMETERS (SATURATING INTENSITY, MODULATION DEPTH) UNDER DIFFERENT CASE

Case	Saturating intensity (MW/cm^2)	Modulation depth
Case 1	103.1	40.01%
Case 2	102.2	40.88%
Case 3	105.6	39.47%
Case 4	107.7	39.35%
Fig. 2b	101.8	41.20%

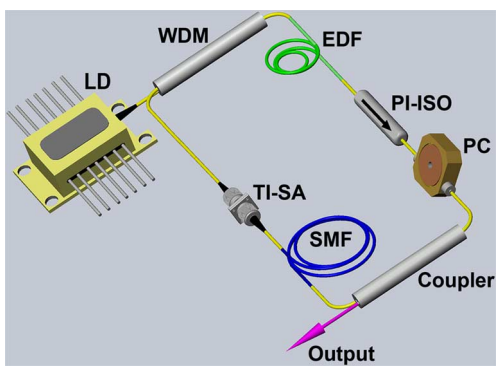

Fig. 4. Schematic of the TI-SA Q-switched fiber ring laser: WDM (wavelength division multiplexer), EDF (erbium-doped fiber), PC (polarization controller), PI-ISO (polarization-independent isolator isolator), SMF (single mode fiber) and TI-SA (topological insulator saturable absorber).

the TI-SA was spliced into the laser cavity. Q-switching of the laser occurred at an incident pump power of 41.3 mW. Fig. 5 summarizes the characteristics of the Q-switched pulses emitted from the fiber laser at a pump power of 68.4 mW. A typical stable Q-switched pulse train of the fiber laser with a repetition rate of 8.865 kHz is shown in Fig. 5(a). The individual pulse has a nearly uniform intensity distribution that is absence of intensity modulation. Fig. 5(b) shows the zoom-in of a single pulse, from which the pulse duration is inferred to be about 14 μs and the pulse has a symmetric intensity profile. The optical spectrum of the Q-switched pulses is shown in Fig. 5(c). It has a 3-dB spectral bandwidth of 0.88 nm and the central wavelength is 1565.14 nm. At a fixed cavity polarization setting, through continuously increasing the pump power, the pulse repetition increased while the pulse train still remained a uniform intensity distribution without obvious fluctuation, as shown in Fig. 5(d). These experimental results show a high passive Q-switching performance of the fiber laser enabled by Bi_2Se_3 saturable absorber.

The relations between the output average power, repetition rate of the Q-switched pulses, and pulse duration of the Q-switched pulses with respect to different incident pump power are summarized in Fig. 6. In Fig. 6(a), the output average power increased almost linearly with the incident pump power, and the single-pulse energy changed between 11.4 and 13.3 nJ. Noting that the minimum intensity value of Q-switched pulse was non-zero, moreover, chaos like continuous wave (CW) sat upon the pedestal, and therefore we believe that a CW component probably coexists on the spectrum of Q-switched pulse that may degrade the optical-optical conversion efficiency. Fig. 6(b) shows the repetition rate and duration of the Q-switched pulses

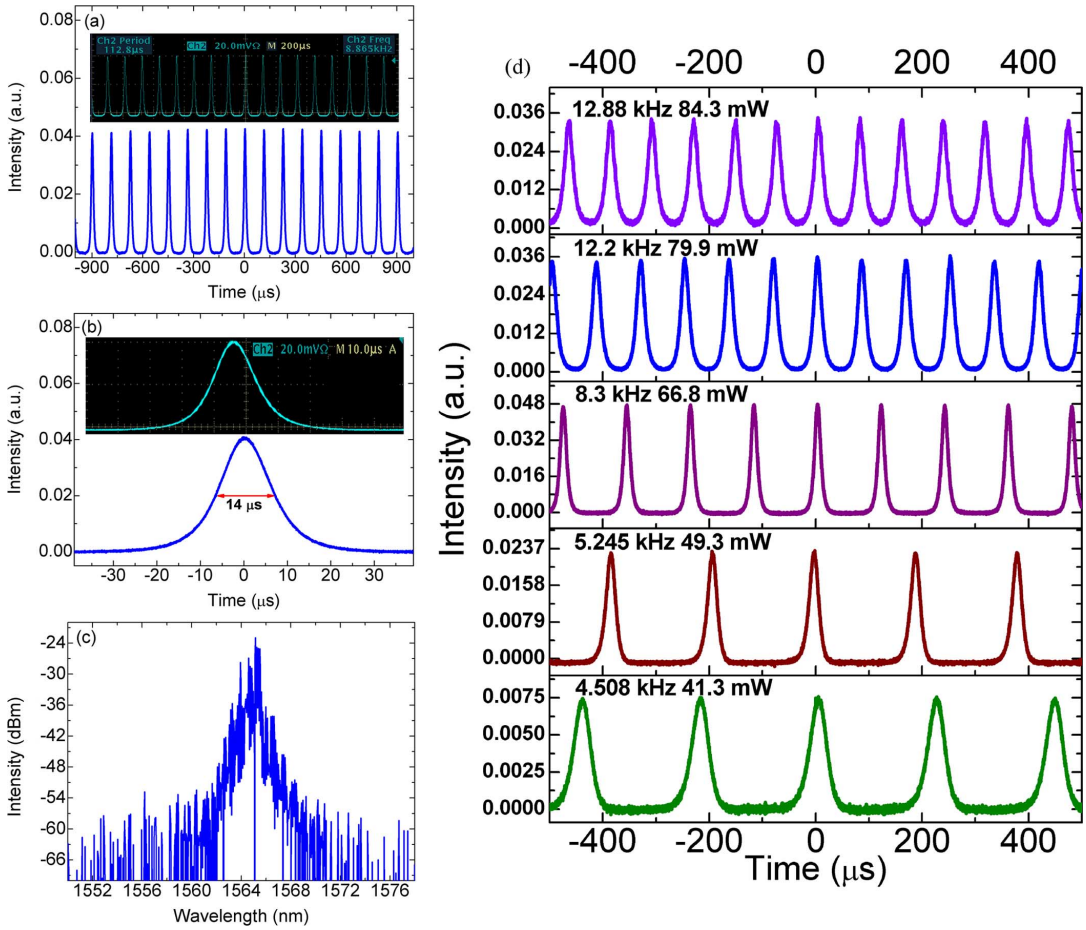

Fig. 5. (a) A typical Q-switched pulse train, (b) single pulse profile and (c) the corresponding output spectrum of the fiber laser obtained at a pump power of 68.4 mW. (d) The various pulse trains obtained under different pump powers.

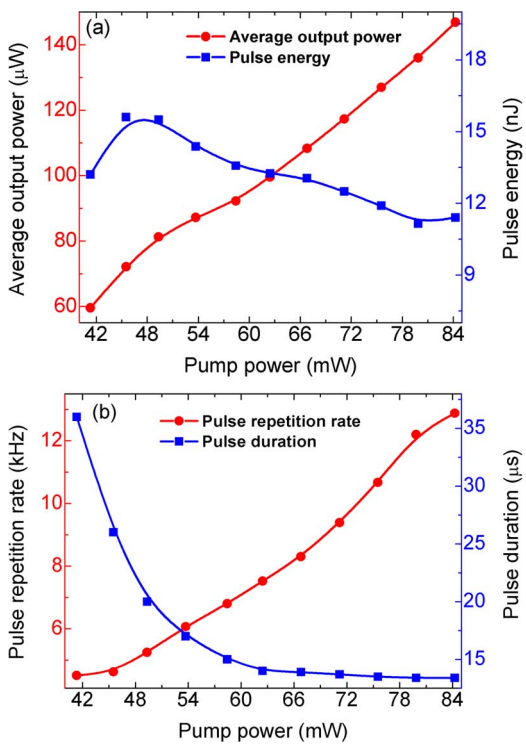

Fig. 6. (a) Output average power and pulse energy, (b) Pulse repetition rate and duration versus incident pump power.

with the incident pump power as it increased from 41.3 mW to 84.3 mW. The repetition rate of the Q-switched pulses increased near linearly from 4.508 to 12.88 kHz, but the pulse duration decreased from 36 to 13.4 μs non- linearly. But once the pump power exceeded 62.5 mW it kept almost constant.

The power achieved by the Q-switched laser is about 15 nJ, corresponding to 19 mJ/cm^2 for the mode field diameter of 10 microns of the SMF. Therefore, the pulse energy in the Q-switched fiber laser cavity is 190 mJ/cm^2. Noting that the saturating intensity of our saturable absorber is 100 MW/cm^2 corresponding to saturating energy of 0.2 mJ/cm^2, it is about three orders of magnitude lower than the energy of Q-switched pulses achieved. This means that the topological insulator saturable absorber operates in the over saturation regime where the pulsed operation can be more stable, which is quite a common nonlinear phenomena in a fiber laser.

Except the pump power, the cavity birefringence also played a central role on the passive Q-switching operation. This can be understood as follows. Cavity birefringence could induce an artificial comb filter effect in a fiber laser cavity, as pointed out in [31]. In a weakly-birefringent fiber laser, the cavity birefringence induced filtering effect is relatively weak and can be ignored because of its large filter bandwidth. However, in a highly birefringent fiber cavity, the cavity birefringence induced filtering effect can no longer be ignored, as in the case the laser oscillation wavelength is determined by the combined

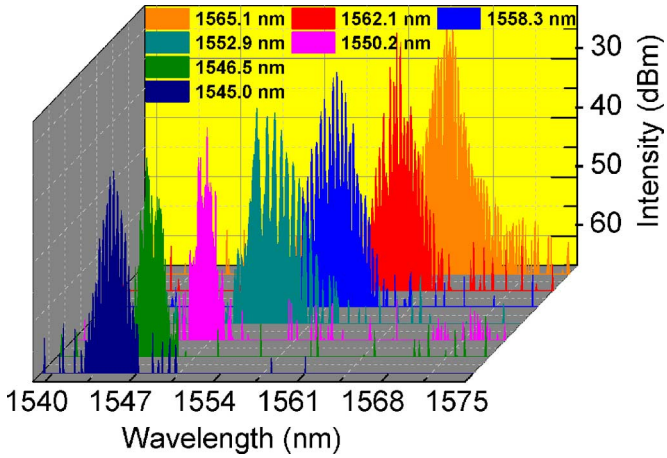

Fig. 7. Output spectra of the laser as the intracavity birefringence is changed.

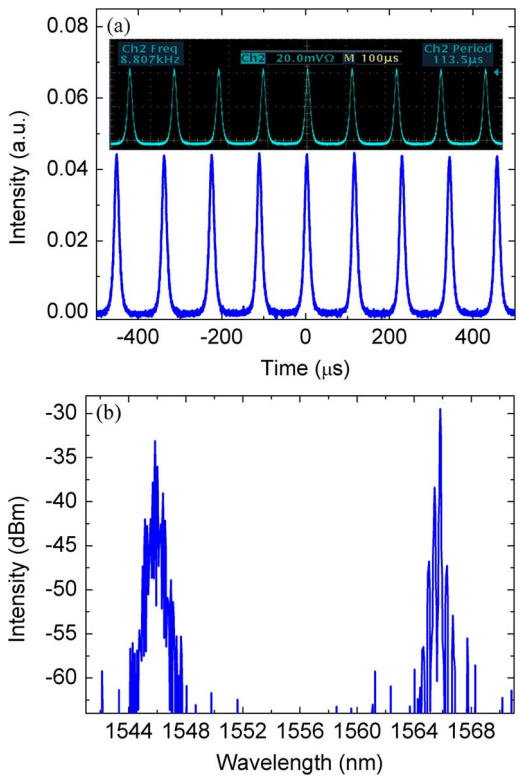

Fig. 8. Pulse trains (a) and spectrum (b) of the dual wavelength Q-switched operation of the laser.

action of the spectral profile of the erbium-doped fiber and the loss spectral profile of the birefringence induced filter that varies with the cavity birefringence. To take advantage of the cavity birefringence induced filtering effect, the same fiber laser cavity is forced to operate in a high-birefringence regime through over-bending the optical fibers looped in the PCs. In such a way an artificial cavity birefringence filter therefore was formed. Changing the strength of the cavity birefringence allows one to tune the Q-switched pulse wavelength. Fig. 7 shows the wavelength tuning of the Q-switched pulses as the intra-cavity PCs were continuously rotated while all the other cavity parameters were unchanged. As can be seen in Fig. 7, the central wavelength of the Q-switched pulses can be tuned from 1565.1 to 1545.0 nm. During the wavelength tuning the Q-switching pulses could be always observed. Even a dual wavelength Q-switched operation with wavelength at 1545.85 and 1565.84 nm respectively was observed by adjusting PC, as shown in Fig. 8(b). Fig. 8(a) is the corresponding Q-switched pulses. Experimentally, we noted that at the longest wavelength 1565.1 nm, the output average power is 112 μW. Output laser power decreases gradually if the wavelength is shifted towards the short wavelength, and at the shortest wavelength of 1545 nm, the output power is about 99 μW.

III. Conclusion

We have reported an erbium-doped Q-switched all-fiber laser with topological insulator Bi_2Se_3 nano-platelets as the saturable absorber. Stable Q-switched pulses with a repetition rate of 8.865 kHz, pulse duration of 14 μs and central wavelength at 1565.14 nm have been directly generated from the fiber laser. Through deliberately increasing the cavity birefringence, e.g., by bending the optical fibers looped in the polarization controllers, we could tune the wavelength of the Q-switched pulses over a range of 20 nm from 1565.1 to 1545.1 nm. Even a dual-wavelength Q-switched operation with oscillating wavelength at 1545.85 and 1565.84, respectively, was experimentally obtained. Our experimental results clearly show that topological insulator Bi_2Se_3 nano-platelets possess saturable absorption, which can be exploited for the pulsed laser applications.

References

[1] X. Zhang, J. Wang, and S. C. Zhang, "Topological insulators for high-performance terahertz to infrared applications," *Phys. Rev. B*, vol. 82, no. 24, p. 245107, Dec. 2010.

[2] J. W. Mclver, D. Hsieh, H. Steinberg, P. Jarillo-Herrero, and N. Gedik, "Control over topological insulator photocurrents with light polarization," *Nat. Nanotech.*, vol. 7, no. 2, pp. 96–100, Dec. 2012.

[3] H. Tang, D. Liang, R. L. Qiu, and X. P. Gao, "Two-dimensional transport-induced linear magneto-resistance in topological insulator Bi_2Se_3 nanoribbons," *ACS Nano*, vol. 5, no. 9, pp. 7510–7516, Jul. 2011.

[4] D. A. Abanin and D. A. Pesin, "Ordering of magnetic impurities and tunable electronic properties of topological insulators," *Phys. Rev. Lett.*, vol. 106, no. 13, p. 136802, Mar. 2011.

[5] M. Z. Hossain, S. L. Rumyantsev, K. M. Shahil, D. Teweldebrhan, M. Shur, and A. A. Balandin, "Low-frequency current fluctuations in Graphene-like exfoliated thin-films of bismuth selenide topological insulators," *ACS Nano*, vol. 5, no. 4, pp. 2657–2663, Mar. 2011.

[6] H. Yuan, H. Liu, H. Shimotani, H. Guo, M. Chen, Q. Xue, and Y. Iwasa, "Liquid-gated ambipolar transport in ultrathin films of a topological insulator Bi_2Te_3," *Nano Lett.*, vol. 11, no. 7, pp. 2601–2605, Jun. 2011.

[7] Vobornik, U. Manju, J. Fujii, F. Borgatti, P. Torelli, D. Krizmancic, Y. S. Hor, R. J. Cava, and G. Panaccione, "Magnetic proximity effect as a pathway to spintronic applications of topological insulators," *Nano Lett.*, vol. 11, no. 10, pp. 4079–4082, Aug. 2011.

[8] H. Zhang, C. X. Liu, X. L. Qi, X. Dai, Z. Fang, and S. C. Zhang, "Topological insulators in Bi_2Se_3, Bi_2Te_3 and Sb_2Te_3 with a single Dirac cone on the surface," *Nat. Phys.*, vol. 5, pp. 438–442, May 2011.

[9] Y. S. Hor, A. Richardella, P. Roushan, Y. Xia, J. G. Checkelsky, M. Z. Hasan, N. P. Ong, A. Yazdani, and R. J. Cava, "P-type Bi_2Se_3 for topological insulator and low-temperature thermoelectric applications," *Phys. Rev. B*, vol. 79, no. 19, p. 195208, May 2009.

[10] S. Cho, N. P. Butch, J. Paglione, and M. S. Fuhrer, "Insulating behavior in ultrathin bismuth selenide field effect transistors," *Nano Lett.*, vol. 11, no. 5, pp. 1925–1927, Apr. 2011.

[11] L. G. Luo and P. L. Chu, "Passive Q-switched erbium-doped fibre laser with saturable absorber," *Opt. Commun.*, vol. 161, no. 4, pp. 257–263, Mar. 1999.

[12] A. V. Kir'yanov, N. N. Il'ichev, and Y. O. Barmenkov, "Excited-state absorption as a source of nonlinear thermo-induced lensing and self-Q-switching in an all-fiber Erbium laser," *Laser Phys. Lett.*, vol. 1, no. 4, pp. 194–198, Mar. 2004.

[13] V. N. Filippov, A. N. Starodumov, and A. V. Kir'yanov, "All-fiber passively Q-switched low-threshold Erbium fiber laser," *Opt. Lett.*, vol. 26, no. 6, pp. 343–345, Mar. 2001.

[14] L. Pan, I. Utkin, and R. Fedosejevs, "Passively Q-switched ytterbium -doped double-clad fiber laser with a Cr^{4+}: YAG saturable absorber," *IEEE Photon. Technol. Lett.*, vol. 19, no. 24, pp. 1979–1981, Dec. 2007.

[15] J. B. Lecourt, G. Martel, M. Guezo, C. Labbe, and S. Loualiche, "Erbium-doped fiber laser passively Q-switched by an InGaAs/InP multiple quantum well saturable absorber," *Opt. Commun.*, vol. 263, no. 1, pp. 71–83, Jul. 2006.

[16] D. P. Zhou, L. Wei, B. Dong, and W. K. Liu, "Tunable passively Q-switched erbium-doped fiber laser with carbon nanotubes as a saturable absorber," *IEEE Photon. Technol. Lett.*, vol. 22, no. 9, pp. 9–11, Jan. 2010.

[17] Z. T. Wang, Y. Chen, C. J. Zhao, H. Zhang, and S. C. Wen, "Switchable dual-wavelength synchronously Q-switched erbium-doped fiber laser based on graphene saturable absorber," *IEEE Photon. J.*, vol. 4, no. 3, pp. 869–876, Jun. 2012.

[18] Y. M. Chang, H. Kim, J. H. Lee, and Y. W. Song, "Multilayered graphene efficiently formed by mechanical exfoliation for nonlinear saturable absorbers in fiber mode-locked lasers," *Appl. Phys. Lett.*, vol. 97, no. 21, p. 211102, Nov. 2012.

[19] H. Kim, J. Cho, S. Y. Jang, and Y. W. Song, "Deformation-immunized optical deposition of graphene for ultrafast pulsed lasers," *Appl. Phys. Lett.*, vol. 98, no. 2, p. 021104, Jan. 2011.

[20] A. Martinez, K. Fuse, and S. Yamashita, "Mechanical exfoliation of graphene for the passive mode-locking of fiber lasers," *Appl. Phys. Lett.*, vol. 99, no. 12, p. 121107, Sep. 2012.

[21] A. Martinez, K. Fuse, B. Xu, and S. Yamashita, "Optical deposition of graphene and carbon nanotubes in a fiber ferrule for passive mode-locked lasing," *Opt. Exp.*, vol. 18, no. 22, pp. 23054–23061, Oct. 2010.

[22] Z. Q. Luo, M. Zhou, D. D. Wu, C. C. Ye, J. Weng, J. Dong, H. Y. Xu, and L. J. Chen, "Graphene-induced nonlinear four-wave-mixing and its application to multiwavelength Q-switched rare-earth-doped fiber lasers," *J. Lightw. Technol.*, vol. 29, no. 18, pp. 2732–2739, Sep. 2011.

[23] S. B. Lu, C. J. Zhao, Y. H. Zou, S. Q. Chen, Y. Chen, Y. Li, H. Zhang, S. C. Wen, and D. Y. Tang, "Third order nonlinear optical property of Bi_2Se_3," *Opt. Exp.*, vol. 21, no. 2, pp. 2072–2082, Jan. 2013.

[24] C. J. Zhao, Y. H. Zou, Y. Chen, Z. T. Wang, S. B. Lu, H. Zhang, S. C. Wen, and D. Y. Tang, "Wavelength-tunable picosecond soliton fiber laser with Topological Insulator: Bi_2Se_3 as a mode locker," *Opt. Exp.*, vol. 20, no. 25, pp. 27888–27895, Dec. 2012.

[25] C. J. Zhao, H. Zhang, X. Qi, Y. Chen, Z. T. Wang, S. C. Wen, and D. Y. Tang, "Ultra-short pulse generation by a topological insulator based saturable absorber," *Appl. Phys. Lett.*, vol. 101, no. 21, p. 211106, Nov. 2012.

[26] P. H. Tang, X. Q. Zhang, C. J. Zhao, Y. Wang, H. Zhang, D. Y. Shen, S. C. Wen, D. Y. Tang, and D. Y. Fan, "Topological insulator: Bi_2Te_3 saturable absorber for the passive Q-switching operation of an in-band pumped 1645-nm Er:YAG ceramic laser," *IEEE Photon. J.*, vol. 5, no. 2, p. 1500707, Apr. 2013.

[27] J. Zhang, Z. Peng, A. Soni, Y. Zhao, Y. Xiong, B. Peng, J. B. Wang, M. S. Dresselhaus, and Q. Xiong, "Raman spectroscopy of few-quintuple layer topological insulator Bi_2Se_3 nanoplatelets," *Nano Lett.*, vol. 11, no. 6, pp. 2407–2414, May 2012.

[28] W. Richter and C. R. Becker, "A Raman and far-infrared investigation of phonons in the rhombohedral V_2-VI_3 compounds Bi_2Te_3, Bi_2Se_3, Sb_2Te_3 and $Bi_2(Te_{1-x}Se_x)_3 (0 < x < 1)$, $(Bi_{1-y}Sb_y)_2Te_3 (0 < y < 1)$," *Phys. Stat. Sol. B*, vol. 84, no. 2, pp. 619–628, Feb. 2006.

[29] D. S. Kong and Y. Cui, "Opportunities in chemistry and materials science for topological insulators and their nanostructures," *Nat. Chem.*, vol. 3, no. 11, pp. 845–849, Oct. 2012.

[30] A. Roberts, D. Cormode, C. Reynolds, T. N. Illige, B. J. LeRoy, and A. S. Sandhu, "Response of graphene to femtosecond high-intensity laser irradiation," *Appl. Phys. Lett.*, vol. 99, no. 5, p. 051912, Aug. 2011.

[31] H. Zhang, D. Y. Tang, X. Wu, and L. M. Zhao, "Multi-wavelength dissipative soliton operation of an erbium-doped fiber laser," *Opt. Exp.*, vol. 17, no. 15, pp. 12692–12697, July 2009.

Author biographies not included at authors' request due to space constraints.